Graphene Oxide-Coated Quartz Crystal Microbalance for Bioparticle Detection (A Case Study for Bacillus sp.)

Budianto, Arif
Faculty of Natural Science and Mathematics, University of Brawijaya

Arinto Yudi Ponco Wardoyo
Faculty of Natural Science and Mathematics, University of Brawijaya

Masruroh
Faculty of Natural Science and Mathematics, University of Brawijaya

Hari Arief Dharmawan
Faculty of Natural Science and Mathematics, University of Brawijaya

他

https://doi.org/10.5109/6781066

Graphene Oxide-Coated Quartz Crystal Microbalance for Bioparticle Detection (A Case Study for *Bacillus sp.*)

Arif Budianto[1,2], Arinto Yudi Ponco Wardoyo[1,*], Masruroh[1], Hari Arief Dharmawan[1], Kasnawi Al Hadi[1,2], Laili Mardiana[1,2]

[1]Faculty of Natural Science and Mathematics, University of Brawijaya, Indonesia
[2]Faculty of Natural Science and Mathematics, University of Mataram, Indonesia

*Author to whom correspondence should be addressed:
E-mail: a.wardoyo@ub.ac.id

Abstract: Bioparticle concentration can be measured using many techniques, such as mass spectroscopy, light scattering, and fluorescent tracking. Due to some instrument limitations, high cost, low sensitivity-selectivity level, and performance development needs, there is a need to develop a new sensing technique with higher performance. This study used quartz crystal microbalance (QCM) and graphene oxide (GO) as the selective coating materials. For this purpose, two different sensors were tested: uncoated QCM and GO-coated QCM. The sensor performances were tested inside an exposure chamber by exposing the sensors to different bacteria samples: *B. pasteurii*, *B. sphaericus*, and *B. cereus*. The sensor's frequency shift was counted using a frequency counter, while the sample concentration was measured using a Digital Dust Monitor. The results show that the sensors work well in detecting *Bacillus sp.* samples with sensitivities of 0.24 to 0.35 Hz.µg^{-1}. The developed sensors have a response time of <96 s, with a linearity of 95%. The best response is obtained from the coated QCM using *B. pasteurii*. The coated QCM performs better than the uncoated QCM, indicated by better linearity, response time, and sensitivity.

1. Introduction

Particulate matter (PM) is a mixture of solid particles and droplets that are suspended in ambient air and is also known as the main contributor to air pollution[1]. In terms of the existence of biological substances, PM generally is categorized into bioparticle and non-bioparticle. According to the size distribution, PM is classified into $PM_{0.1}$, $PM_{2.5}$, and PM_{10}. Ultrafine particle ($PM_{0.1}$) has a diameter of < 0.1 µm, determined as the smallest particulate matter with the highest impact on human health[1]. $PM_{2.5}$, a fine particle, has a bigger diameter than an ultrafine particle, between 0.1 to 2.5 µm[2]. The biggest particulate matter is a coarse particle or PM_{10}, which has an aerodynamic diameter of 2.5 µm to 10 µm[3]. The different substances and size distribution of particulate matter make different characteristics and health impacts on humans[1,4].

Bioparticle is a kind of particulate matter consisting of fungal spores, bacteria, and viruses in fine and ultrafine particles[5,6]. Bioparticles can easily be dispersed in ambient air as atmospheric particles, airborne particles, or bioaerosol. They can be found in indoor and outdoor areas, such as medical rooms, isolation rooms, small rooms, and even house[5,7,8]. Bacteriophage and SARS-CoV-2

(coronavirus)[9,10] are examples of bioparticles in terms of virus type. In bacteria class, bioparticle consists of many genera, including *Bacillus cereus*, *Bacillus infantis*, *Bacillus marisflavi*, *Bacillus subtilis*, and *Bacillus atrophaeus*[11]. *Cladosporium* spp., *Mycosphaerella* spp., and *Penicillium* spp. are examples of fungal bioparticles which can be found both in indoor and outdoor environments[8].

Bioparticle concentration can be measured using some techniques, such as fluorescent tracking, lightwave principle, spectroscopy method, and biomolecular reaction. Fluorescent tracking and lightwave principle, a physics approach, counts the bioparticle concentrations using optical particle counting or light scattering sensors (refraction, reflection, or diffraction) and fluorescent tracking[9,10,12]. This technique performs a fast measuring method without identification or specific bioparticle types. Another study used UV-APS (ultraviolet aerodynamic particle sizer) to measure bioparticles with an aerodynamic diameter < 1 µm[13]. These measurement systems are not portable, are high-cost, generally use indirect measurement, and need extra maintenance or specific attention. Other measurements can be done using spectroscopic techniques, such as Energy Dispersive X-

ray spectroscopy, Raman-spectroscopy, and mass spectrometry. These methods have been widely used to quantify many bioparticles, such as airborne magnetic nanoparticles[14], bacteria[11], bacteria from fish muscle[15], and pathogenic airborne viruses[10]. Both spectrometry and spectroscopy are indeed widely used for bioparticle measurement devices. However, spectrometry and spectroscopy are not portable devices and need a supporting ecosystem, such as a controlled room and a well-trained operator. In biology science, RT-PCR (real-time polymerase chain reaction) technique has been used widely to quantify and detect specific microorganisms in environmental samples[16,17]. However, this technique needs supporting technology (*e.g.,* special laboratories, specific rooms, reagents, and other devices) and trained operators.

Quartz crystal microbalance (QCM) is a unique crystal that works for gravimetric measurements based on frequency shift and mass loading effect[18,19]. According to Sauerbrey's equation, this crystal has a fundamental frequency, while the frequency shift is linear to the deposited mass on the crystal surface[20]. The interaction between the deposited mass and QCM's surface is also influenced by the coating material applied to the surface area and other important parameters[21]. As supported by previous studies, the exact coating material will make the highly selective binding of the QCM as a specific sensor (not just a crystal)[22,23]. In other words, a bare QCM needs a correct coating material when being developed as a specific sensor.

Graphene oxide (GO), a graphene derivative, can be developed as a QCM coating material, resulting in a GO-coated QCM. GO has a high specific surface area, easy stacking, easy functionalization, good hydrophilicity, and dispersion stability, making it suitable for coating material or thin film in surface modification[24]. GO also has a good mechanical modulus which may cause a small probability of the swelling effect due to the over-mass loading impact (false QCM'S response due to over-deposited mass) that influences the QCM response[25], such as studying for formaldehyde concentration[26], gas sensor[27], and relative humidity sensor[18].

According to the previous explanation, GO-coated QCM has the potential to be developed as a bioparticle sensor. It will be a novel method or measurement device for measuring bioparticle concentration based on the gravimetric principle. It will provide better sensitivity and accuracy, faster response, portability, and inexpensive materials than other measurement devices. Hence, this study is aimed to develop a new bioparticle detection system using a GO-coated QCM. This study also investigates the performance comparison between uncoated and GO-coated QCMs in detecting bioparticles, with a specific case in bacteria type. For a case study and also as a preliminary study for the development of a more complex bioparticle counter, *Bacillus sp.* was chosen due to its important and typical bacterial strain found as

airborne particles in the indoor atmosphere.

2. Materials and Methods

2.1 Sensor preparation

Two different QCMs (diameter = 0.87 cm, electrode area (A) = 0.196 cm^2) were used as the sensors: Q1 (bare QCM) and Q2 (GO-coated QCM). Q2 sensor was developed by coating the surface of a bare QCM using GO solution (2 mg.mL^{-1}, dissolved in deionized water, purity = 99%). A spin coating method (speed = 700 RPM) was used for the coating process to coat the top surface of a silver-coated QCM with an f_0 (fundamental frequency) of 5 MHz. Thus, the QCM was coated with the as-prepared GO for 3 minutes. This coating duration was selected due to the best deposition characteristics. After that, the prepared sensors were installed inside a sensing box connected to the frequency driver and counter as the sensing analysis system (Fig. 1).
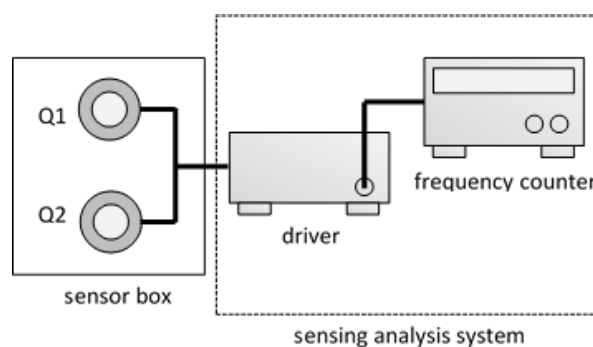

Fig. 1: Sensors configuration inside the sensing box.

2.2 Bioparticle concentration measurement

Bacillus sphaericus (B1), *Bacillus pasteurii* (B2), and *Bacillus cereus* (B3) were used as bioparticle samples. These samples were cultivated and isolated on glass Petri dishes containing Potato-Dextrose Agar (Merck, 1.10130.0500). They were incubated at 25°C for a week inside a chamber. These samples were chosen for safety purposes, as they were categorized as safe microorganisms from their species.

On the 8th day, each sample was placed inside an exposure chamber (volume V = 2,250 cm^3) connected to a suction pump (airspeed v = 200 cm.s^{-1}), a HEPA filter, and a digital Dust Monitor (Kanomax, model 3443) (Fig. 2). The suction pump (brushless DC motor) was used to efficiently inject fresh air into the chamber and disperse the bioparticles from the sample inside the chamber[28,29]. The Digital Dust Monitor measured bioparticle concentration (C_n) for a certain sampling time (t). Related to the pump's airspeed (v), outlet area (A, 0.28 cm^2), and chamber volume (V), the sample injection was conducted for 40 seconds (t_i) since:

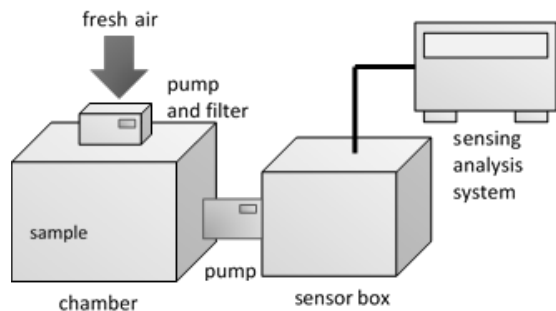$$t_i = \frac{V}{A \cdot v} \tag{1}$$

Fig. 2: Schematic diagram of bioparticle concentration.

2.3 Sensor test

A similar method of concentration measurement was applied using the developed system. The sensing box and the sensing analysis system were connected to the chamber, filter, and pump (Fig. 2), replacing the function of the Digital Dust Monitor. The sensing analysis system measured the frequency shift (Δf). Related to the Sauerbrey equation (Eq. 2), Δf is linear to the deposited bioparticle mass (Δm) on the sensors' surface. The measured bioparticle concentration from the sensors (C_c) was calculated using Eq. 3[30].

$$\Delta m = -\ \frac{A\sqrt{\rho\,\mu}}{2\,f_0^2}\ .\ \Delta f \qquad (2)$$

$$C_c = \frac{\Delta m}{V} \qquad (3)$$

Constants μ and ρ are shear modulus (2.947×10^{11} g.cm^{-1}.s^{-2}) and crystal density (2.684 g.cm^{-3}). The measured (C_n) and calculated bioparticle concentrations (C_c) were used to calculate the sensor performance, including sensitivity (S), accuracy (A), and linearity (R^2). The sensitivity level was calculated using the equation:
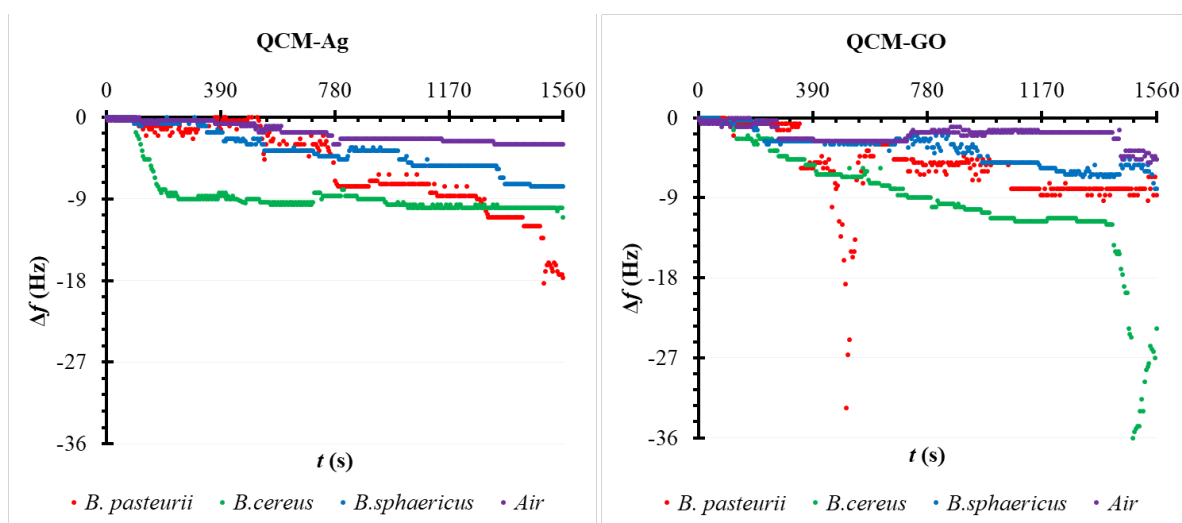
$$S = \frac{\Delta f}{C_n} \qquad (4)$$

2.4 Statistical analysis

There were three replicates ($n = 3$) for each datum point in all measurements. All data are interpreted as the mean $\pm$ standard deviation (SD). A Student's t-test calculates the significance, while differences were considered significant at $p \leq 0.05$.

3. Results

3.1 Bioparticle concentration

Table 1 shows the measured bioparticle concentrations (C_n) inside the chamber (measured by the Digital Dust Monitor as the comparator device). The most concentration is measured from the B3 sample or *Bacillus cereus* (more than 800 µg.m^{-3}). Compared to the control parameter, B4 (fresh air), this concentration is 797 µg.m^{-3} higher. *Bacillus pasteurii* has the second position, 20% smaller than the measured concentration in *Bacillus cereus*. These different concentrations are related to the different bacteria samples. Each bacteria sample has a different biological characteristic. Meanwhile, a significant concentration difference between B1-B3 and B4 confirms that the cultivated bacteria were dispersed in the chamber resulting in bioparticle concentration with certain bacteria as the main contaminants.

Table 1. Bioparticle concentrations.

Code	Samples	C_n (µg.m^{-3})
B1	*Bacillus sphaericus*	444±2
B2	*Bacillus pasteurii*	666±11
B3	*Bacillus cereus*	825±24
B4	Filtered air	28±5

3.2 Frequency Response

The frequency shifts corresponding to different samples using Q1 and Q2 sensors are shown in Fig. 3.

Fig. 3: The frequency shift corresponds to different sensors and bioparticle samples.

According to this figure, in Q1, *Bacillus pasteurii* bonded to the QCM sensor in a big change in the frequency shift Δf (-18 Hz), indicating that the deposited particles are relatively high. The second place is referred to as *Bacillus cereus*, resulting in a frequency shift of -11 Hz, only 3 Hz higher than *Bacillus sphaericus*. The graph shows that *Bacillus sphaericus* generates the lowest response to Q1.

Different results are found in GO-coated QCM or Q2. This sensor has relatively bigger frequency shifts than the uncoated QCM (Q1). The most frequency shift is found in *Bacillus cereus* (-36 Hz). This result is 25 Hz higher than Q1 (-11 Hz). This frequency shift indicates that Q2 has a good response for *Bacillus sphaericus*. *Bacillus cereus* has a continuous trendline. It can be assumed that the sensor was still sensitive to this sample (green dots) regarding the 1560 s of the sampling duration. There is no saturation characteristic, and the sensor could still detect more samples (a longer measurement range).

Interestingly in Q2, the second position is referred to as *Bacillus pasteurii* with a -33 Hz frequency shift. This value is 15 Hz higher than the result of Q1. The trendline indicates good reliability since the frequency shift approaches the initial value. This characteristic might be related to the different interactions between samples and the GO layer.

In contrast, there is no different result between Q1 and Q2 for *Bacillus sphaericus*. For this sample, Q2 only has -8 Hz of frequency shift. All results show a good pattern, whereas the decreasing frequency is consistent in a series of times. Above all, Q2 shows a better Δf consistency than Q1.

3.3 Sensor characteristic

Fig. 4a depicts the sensitivity level of Q2. Q2 has interesting results, with sensitivity levels of 0.24 to 0.35 Hz.µg^{-1} with a low standard deviation. The best sensitivity is obtained at *Bacillus pasteurii* (0.35 Hz.µg^{-1}) with an error value of 34%. The second position is *Bacillus cereus*, with a sensitivity of 0.33±0.08 Hz.µg^{-1} (error value = 25%). *Bacillus sphaericus* generates the smallest sensitivity, showing a level of 0.24 Hz.µg^{-1} (error value = 14%). In contrast, Q1 has a higher value of 0.24 to 0.28 Hz.µg^{-1}. Sensitivity is determined as a better result when the value is lower or when the sensor is reacted to a similar bioparticle concentration. It is also related to system resolution.

This study also investigates the sensor linearity based on bioparticle concentration (Fig. 4b). The calculated particle concentrations (obtained from QCM sensors) show a significant difference compared to the measured ones (measured from the Digital Dust Monitor). As expected, Q2 has better linearity ($R^2 = 0.95$) than Q1 ($R^2 = 0.29$).

The uncoated QCM sensor approaches an exponential function as the best fitting, with a regression coefficient of 0.60. A higher R^2 or regression coefficient indicates no

significant difference between the comparator device and Q2. Meanwhile, Q1 does not show a good performance in terms of linearity and sensitivity.
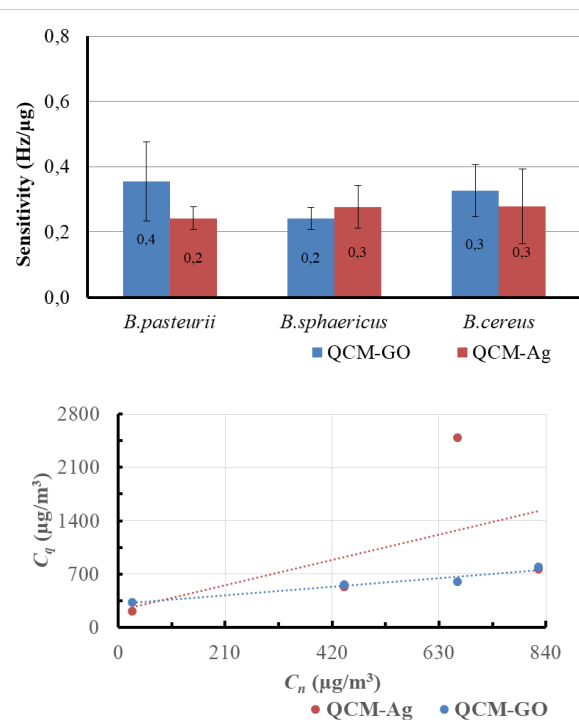

Fig. 4: The sensor sensitivity (a) and linearity (b).

4. Discussion

QCM was used as the sensing element in this study. The main reason is the characteristic of the QCM crystal that works for gravimetric measurements based on frequency change (Δf)[31]. The resonant frequency is related to the deposited particles (Δm) on the crystal surface area A[32]. The QCM performance due to this deposition is influenced by the interaction between the targetted analyte and the coating material on the crystal surface. In this state, the resonant frequency depends on the surface and internal analyte bonds. Thus, the exact coating material will make the highly selective binding of the QCM sensors in the immobilization process[33]. Some previous studies also suggest a specific thin film coating to increase the QCM selectivities for the different analytes[19].

The bare QCM has a lower performance than Q2. This study shows nonsignificant results with high relative errors (>14%) in the sensitivity parameter. These high standard deviations may indicate a great uncertainty in the bare QCMs ($R^2 = 0.2919$). The above data also confirms that Q1 needs a longer time to detect bioparticles (90 to 105 s of response times) than the Q2 sensor. Thus, this lower performance is mainly related to the absence of GO coating. These results also suggest that bare QCM is only a gravimetric crystal that has the potential to be used as a sensor when coated by a specific film.

As expected, the results show that Q2 performs well in sensing bioparticles. The coated QCM has a better

response time, linearity (R^2 = 0.95), and sensitivity than the uncoated one. As seen in Fig. 4, the linearity of Q2 is 0.9505 (much higher than Q1), >60% higher than the bare QCM. This sensor needs <96 s to sense bioparticles, with a sensitivity of 0.24 Hz.µg^{-1} (B1), 0.35 Hz.µg^{-1} (B2), and 0.33 Hz.µg^{-1} (B3). These results confirm the ability of GO as the coating material to bound bacteria *Bacillus sp.*

This study used GO as the coating material to improve the sensitivity and other performance parameters. GO, and other carbon derivatives have good porous layer[34,35]. GO was chosen due to its chemical groups and physical characteristics influencing the sensor's performance[36]. In the case of bioparticle interaction, GO can induce cell damage. This probability is supported by a previous study using *Azotobacter chroococcum*, where GO could break cell walls assigning membrane damage[37]. In the presence of GO, it seemed that the surface of the GO-coated QCM would make contact with the analyte, bind them, and the analytes were embedded within the GO-coated surface. The break of cell walls became evidence of the potential and probable GO toxicity mechanisms again bio-PM analyte[38]. Other previous studies also support the role of GO as an antifungal and antibacterial material by analyzing the reduction in the number of bioparticles[39,40]. Hence, GO thin-film might influence and increase the sensor performance more than uncoated QCM.

5. Conclusion

This study uses graphene oxide as a thin film for QCM crystal. The coated QCM works well as a bioparticle sensor in *Bacillus sp*. The GO-coated QCM has a better performance compared to the bare QCM. The sensitivities of QCM-GO are in the range of 0.24 to 0.35 Hz.µg^{-1}, with a response time and linearity of <96 s and >0.93, consecutively. The uncoated QCM has a lower performance, indicated by lower linearity (0.29), lower sensitivity (0.24-0.28 Hz.µg^{-1}), and longer response time (90 s to 105 s). These results show that GO can be applied as a sensitive coating material to produce a bacteria sensor.

Acknowledgments

Nomenclature

Cn	measured concentration (µg.m^{-3})
Cc	calculated concentration (µg.m^{-3})
A	accuracy (%)
S	sensitivity (Hz.m^3.ug^{-1})
f	frequency (Hz)
Δf	frequency shift (Hz)

References

1) H. Samae, S. Tekasakul, P. Tekasakul, W. Phairuang, M. Furuuchi, and S. Hongtieab, "Particle-bound organic and elemental carbons for source identification of PM < 0.1 µm from biomass combustion," *J. Environ. Sci. (China)*, **113** 385–393 (2022). doi:10.1016/j.jes.2021.06.015.

2) H. Wang, H. Zhang, J. Li, J. Liao, J. Liu, C. Hu, X. Sun, T. Zheng, W. Xia, S. Xu, S. Wang, and Y. Li, "Prenatal and early postnatal exposure to ambient particulate matter and early childhood neurodevelopment: A birth cohort study," *Environ. Res.,* **210** 112946 (2022). doi: 10.1016/j.envres.2022.112946.

3) Y. S. Joo, J. Kim, J. Lee, and I. J. Chung, "Fine particulate matter and depressive symptoms in children: A mediation model of physical activity and a moderation model of family poverty," *SSM - Popul. Heal.*, **17** 101015 (2022). doi: 10.1016/j.ssmph.2021.101015.

4) A. L. Prinz, and D. J. Richter, "Long-term exposure to fine particulate matter air pollution: An ecological study of its effect on COVID-19 cases and fatality in Germany," *Environ. Res.*, **204** 111948 (2022). doi: 10.1016/j.envres.2021.111948.

5) X. Yan, J. Ma, X. Chen, M. Lei, T. Li, and Y. Han, "Characteristics of airborne bacterial communities and antibiotic resistance genes under different air quality levels," *Environ. Int.*, **161** 107127 (2022). doi:10.1016/j.envint.2022.107127.

6) L. E. Breshears, B. T. Nguyen, B. T., S. M. Robles, L. Wu, and J. Y. Yoon, "Biosensor detection of airborne respiratory viruses such as SARS-CoV-2," *SLAS Technol.*, **27** 4–17 (2022). doi: 10.1016/j.slast.2021.12.004.

7) W. B. Chekol, and D. Y. Melesse, "Operating room team safety and perioperative anesthetic management of patients with suspected or confirmed novel corona virus in resource limited settings: A systematic review," *Trends Anaesth. Crit. Care*, **34** 14–22 (2020). doi:10.1016/j.tacc.2020.06.011.

8) A. Núñez, and A. M. García, "Effect of the passive natural ventilation on the bioaerosol in a small room," *Build. Environ.*, **207** 108438 (2022). doi: 10.1016/j.buildenv.2021.108438.

9) J. Ren, M. Tang, and A. Novoselac, "Experimental study to quantify airborne particle deposition onto and resuspension from clothing using a fluorescent-tracking method," *Build. Environ.*, **209** 108580 (2022). doi:10.1016/j.buildenv.2021.108580.

10) J. Bhardwaj, S. Hong, J. Jang, C. H. Han, J. Lee, and J. Jang, "Recent advancements in the measurement of pathogenic airborne viruses," *J. Hazard. Mater.*, **420** 126574 (2021). doi:10.1016/j.jhazmat.2021.126574.

11) M. Y. Ashfaq, D. A. Da'na, and M. A. Al-Ghouti, "Application of MALDI-TOF MS for identification of environmental bacteria: A review," *J. Environ. Manage*., **305**, 114359 (2022). doi:10.1016/j.jenvman.2021.114359.

12) Y. L. Pan, K. Aptowicz, J. Arnold, S. Cheng, A. Kalume, P. Piedra, C. Wang, J. Santarpia, and G. Videen, "Review of Elastic Light Scattering from Single Aerosol Particles and Application in Bioaerosol Detection," *J. Quant. Spectrosc. Radiat. Transf*., **279** 108067 (2022). doi: 10.1016/j.jqsrt.2022.108067.

13) J. H. Tian, C. Yan, Z. A. Nasir, S. G. Alcega, S. Tyrrel, and F. Coulon, "Real time detection and characterisation of bioaerosol emissions from wastewater treatment plants," *Sci. Total Environ*., **721** 137629 (2020). doi:10.1016/j.scitotenv.2020. 137629.

14) C. Martinez-Boubeta, and K. Simeonidis, "Airborne magnetic nanoparticles may contribute to COVID-19 outbreak: Relationships in Greece and Iran," *Environ. Res*., **204** 112054 (2022). doi: 10.1016/j.envres.2021.112054.

15) Z. Chai, and H. Bi, "Capture and identification of bacteria from fish muscle based on immunomagnetic beads and MALDI-TOF MS," *Food Chem. X*, **100225** (2022). doi:10.1016/j.fochx.2022.100225.

16) S. Elli, F. Blasi, B. Brignolo, F. Ceriotti, A. Gori, A. Piatti, M. Solbiati, and G. Costantino, "Diagnostic accuracy of rapid antigen test for COVID-19 in an emergency department," *Diagn. Microbiol. Infect. Dis*., **102** 115635 (2022). doi: 10.1016/j.diagmicrobio.2022.115635.

17) H. Ilkhani, N. Hedayat, and S. Farhad, "Novel approaches for rapid detection of COVID-19 during the pandemic: A review," *Anal. Biochem*., **634** 114362 (2021). doi:10.1016/j.ab.2021.114362.

18) R. Yi, B. Peng, Y. Zhao, D. Nie, L. Chen, and L. Zhang, "Quartz crystal microbalance humidity sensors based on Structured Graphene Oxide membranes with magnesium ions: Design, mechanism and performance," *Membranes (Basel)*., **12** 125 (2022). doi:10.3390/membranes12020125.

19) M. Yılmaz, M. Bakhshpour, I. Göktürk, A. K. Pişkin, and A. Denizli, "Quartz crystal microbalance (QCM) based biosensor functionalized by her2/neu antibody for breast cancer cell detection," *Chemosensors*, **9** (2021). doi: 10.3390/chemosensors9040080.

20) N. Liu, X. Xiang, M. Sun, P. Li, H. Qin, H. Liu, Y. Zhou, L. Wang, L. Wu, and J. Zhu "Flexible hydrogel non-enzymatic QCM sensor for continuous glucose monitoring," *Biosens Bioelectron. X*, **10** 100110 (2022). doi: 10.1016/j.biosx.2022.100110.

21) C. E. Kirimli, E. Elgun, and U. Unal, "Machine learning approach to optimization of parameters for impedance measurements of Quartz Crystal Microbalance to improve limit of detection," *Biosens. Bioelectron. X*, **10** 100121 (2022). doi: 10.1016/j.biosx.2022.100121.

22) I. R. Jang, S. I. Jung, G. Lee, I. Park, S. B. Kim, and H. J. Kim, "Quartz crystal microbalance with thermally-controlled surface adhesion for an efficient fine dust collection and sensing," *J. Hazard. Mater*., **424** 127560 (2022). doi:10.1016/j.jhazmat. 2021. 127560.

23) T. Liangsupree, E. Multia, P. Forssén, T. Fornstedt, and M. L. Riekkola, "Kinetics and interaction studies of anti-tetraspanin antibodies and ICAM-1 with extracellular vesicle subpopulations using continuous flow quartz crystal microbalance biosensor," *Biosens Bioelectron*., **206** 114151 (2022). doi:10.1016/j.bios.2022.114151.

24) H. Y. Mohammed, M. A. Farea, P. W. Sayyad, N. N. Ingle, T. Al-Gahouari, M. M. Mahadik, G. A. Bodkhe, S. M. Shirsat, and M. D. Shirsat, "Selective and sensitive chemiresistive sensors based on polyaniline/graphene oxide nanocomposite: A cost-effective approach," *J. Sci. Adv. Mater. Devices*, **7** 100391 (2022). doi:10.1016/j.jsamd.2021.08.004.

25) C. Y. Ho, and Y. S. Wu, "Diamine decorated graphene oxide film on quartz crystal microbalance for humidity-sensing analysis," *Appl. Surf. Sci*., **510** 145257 (2020). doi:10.1016/j.apsusc.2020.145257.

26) M. Yang, and J. He, "Graphene oxide as quartz crystal microbalance sensing layers for detection of formaldehyde," *Sensors Actuators, B Chem*., **228** 486–490 (2016). doi:10.1016/j.snb.2016.01.046.

27) S. Jayawardena, A. Kubono, R. M. G. Rajapakse, and M. Shimomura, "Effect of titanium precursors used in the preparation of graphene oxide/TiO$_2$ composite for gas sensing utilizing quartz crystal microbalance," *Nano-Structures & Nano-Objects*, **28** 100780 (2021). doi:10.1016/j.nanoso.2021. 100780.

28) Safril, Mustofa, M. Zen, F. Sumasto, and M. Wirandi, "Design of cooling system on brushless DC motor to improve heat transfers efficiency," *Evergreen*, **9** 584–593 (2022). doi:10.5109/4794206.

29) A. R. A. Bahar, A. S. Yatim, and E. P. Wijaya, "CFD analysis of Universitas Indonesia psychrometric chamber air loop system," *Evergreen*, **9** 465–469 (2022). doi:10.5109/4794173.

30) G. Sauerbrey, "Verwendung von Schwingquarzen zur Wägung dünner Schichten und zur Mikrowägung," *Zeitschrift für Phys*., **155** 206–222 (1959). doi:10.1007/BF01337937.

31) F. N. Dultsev, and A. V. Tronin, "Rapid sensing of hepatitis B virus using QCM in the thickness shear mode," *Sensors Actuators, B Chem*., **216** 1–5 (2015). doi:10.1016/j.snb.2015.04.027.

32) M. Gianneli, Y. Yan, E. Polo, D. Peiris, T. Aastrup, and K. A. Dawson, "Novel QCM-based Method to Predict in Vivo Behaviour of Nanoparticles," *Procedia Technol*., **27** 197–200 (2017). doi: 10.1016/j.protcy.2017.04.084.

33) L. Wang, R. Wang, F. Chen, T. Jiang, H. Wang, M.

Slavik, H. Wei, and Y. Li, "QCM-based aptamer selection and detection of Salmonella typhimurium," *Food Chem.*, **221** 776–782 (2017). doi: 10.1016/j.foodchem.2016.11.104.

34) V. A. Gandhari, M. S. Perdani, and H. Heri, "Improvement on reusability, storage stability and thermal stability of magnetic graphene oxide-immobilized cholesterol oxidase," *Evergreen*, **9** 500–505 (2022). doi:10.5109/4794178.

35) J. Miyawaki, J. Yeh, H-S. Kil, J-K. Lee, K. Nakabayashi, I. Mochida, and S-H. Yoon, "Influence of pore size and surface functionality of activated carbons on adsorption behaviors of indole and amylase," *Evergreen*, **3** 17–24 (2016). doi:10.5109/1800868.

36) K. Zhang, R. Hu, G. Fan, and G. Li, "Graphene oxide/chitosan nanocomposite coated quartz crystal microbalance sensor for detection of amine vapors," *Sensors Actuators B. Chem.*, **243** 721–730 (2017). doi:10.1016/j.snb.2016.12.063.

37) A. Yilihamu, B. Ouyang, P. Ouyang, Y. Bai, Q. Zhang, M. Shi, X. Guan, and S. T. Yang, "Interaction between graphene oxide and nitrogen-fixing bacterium Azotobacter chroococcum: Transformation, toxicity and nitrogen fixation," *Carbon N. Y.*, **160** 5–13 (2020). doi: 10.1016/j.carbon.2020.01.014.

38) M. Burger, and L. E. Jackson, "Microbial immobilization of ammonium and nitrate in relation to ammonification and nitrification rates in organic and conventional cropping systems," *Soil Biol. Biochem.*, **35** 29–36 (2003). doi: 10.1016/S0038-0717(02)00233-X.

39) H. Wang, G. Li, and A. Fakhri, "Fabrication and structural of the Ag2S-MgO/graphene oxide nanocomposites with high photocatalysis and antimicrobial activities," *J. Photochem. Photobiol. B Biol.*, **207** 111882 (2020). doi: 10.1016/j.jphotobiol.2020.111882.

40) N. S. Ahmad, N. Abdullah, and F. M. Yasin, "Toxicity assessment of reduced graphene oxide and titanium dioxide nanomaterials on gram-positive and gram-negative bacteria under normal laboratory lighting condition," *Toxicol. Reports*, **7** 693–699 (2020). doi:10.1016/j.toxrep.2020.04.015.